

## **Electronic Supplementary Information (ESI)**

### **An Efficient, Rapid, and Non-Centrifuged Synthesis of Nanosized Zeolites by Accelerating Nucleation Rate**

Changsheng Zhang,<sup>a</sup> Qinming Wu,<sup>a</sup> Chi Lei,<sup>a</sup> Shichao Han,<sup>a</sup> Qiuyan Zhu,<sup>a</sup> Stefan Maurer,<sup>b</sup> Daniel Dai,<sup>b</sup> Andrei-Nicolae Parvulescu,<sup>c</sup> Ulrich Müller,<sup>c</sup> Xiangju Meng,<sup>\*a</sup> and Feng-Shou Xiao<sup>\*a</sup>

<sup>a</sup> Key Laboratory of Applied Chemistry of Zhejiang Province, Zhejiang University, Hangzhou 310028, China. \*E-mail: mengxj@zju.edu.cn; fsxiao@zju.edu.cn

<sup>b</sup> BASF Catalysts (Shanghai) Co., Ltd., 239 Luqiao Road, Jinqiao Export Process Zone Pudong New District, Shanghai, 201206, China

<sup>c</sup> BASF SE, GCC/PZ – M311, 67056 Ludwigshafen, Germany

## Supporting Figures

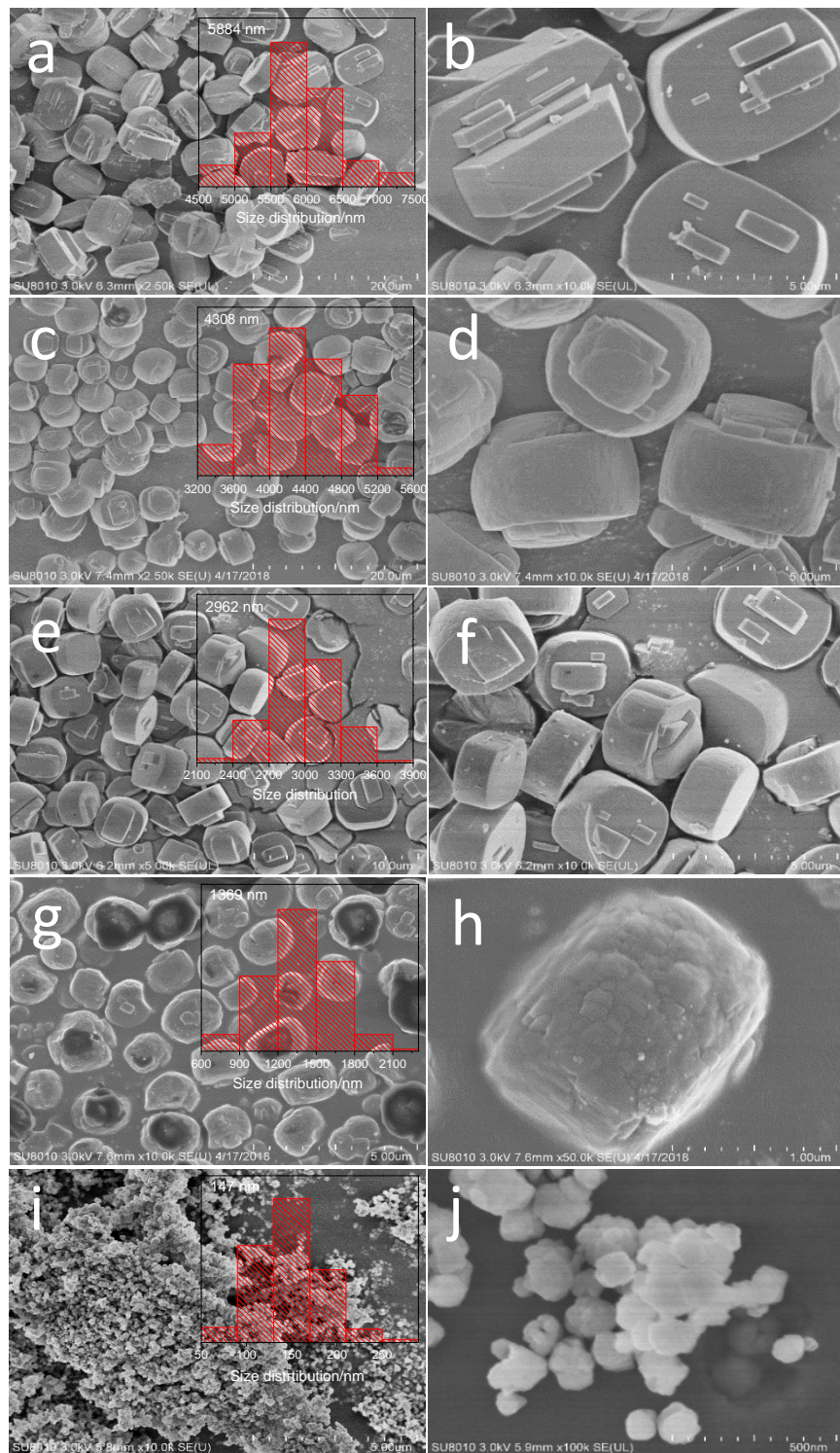


**Fig. S1** SEM images of the ZSM-5 synthesized with H<sub>2</sub>O/SiO<sub>2</sub> ratio at (a,b) 18, (c,d) 12, (e,f) 10, (g,h) 6, (i,j) 2 crystallized at 180 °C (Size distribution of ZSM-5 zeolite obtained by counting number of more than 200 zeolite particles in the SEM images).

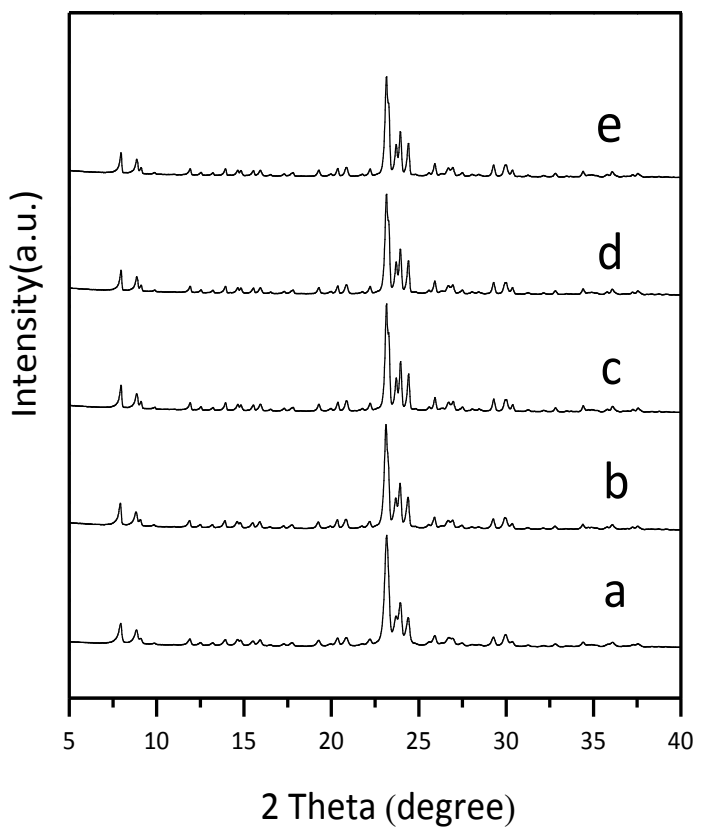


**Fig. S2** XRD patterns of the ZSM-5 synthesized with  $\text{H}_2\text{O}/\text{SiO}_2$  ratio at (a) 2, (b) 6, (c) 10, (d) 12 and (e) 18 crystallized at 180 °C.

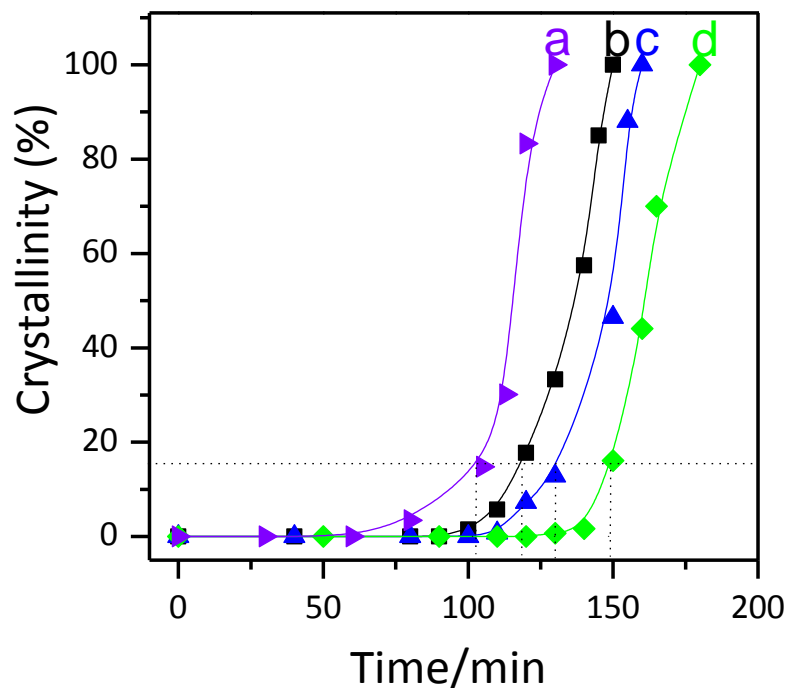


**Fig. S3** Dependences of the ZSM-5 crystallinity on the crystallization time synthesized with H<sub>2</sub>O/SiO<sub>2</sub> ratio at (a) 2, (b) 6, (c) 10, and (d) 18 crystallized at 180 °C.

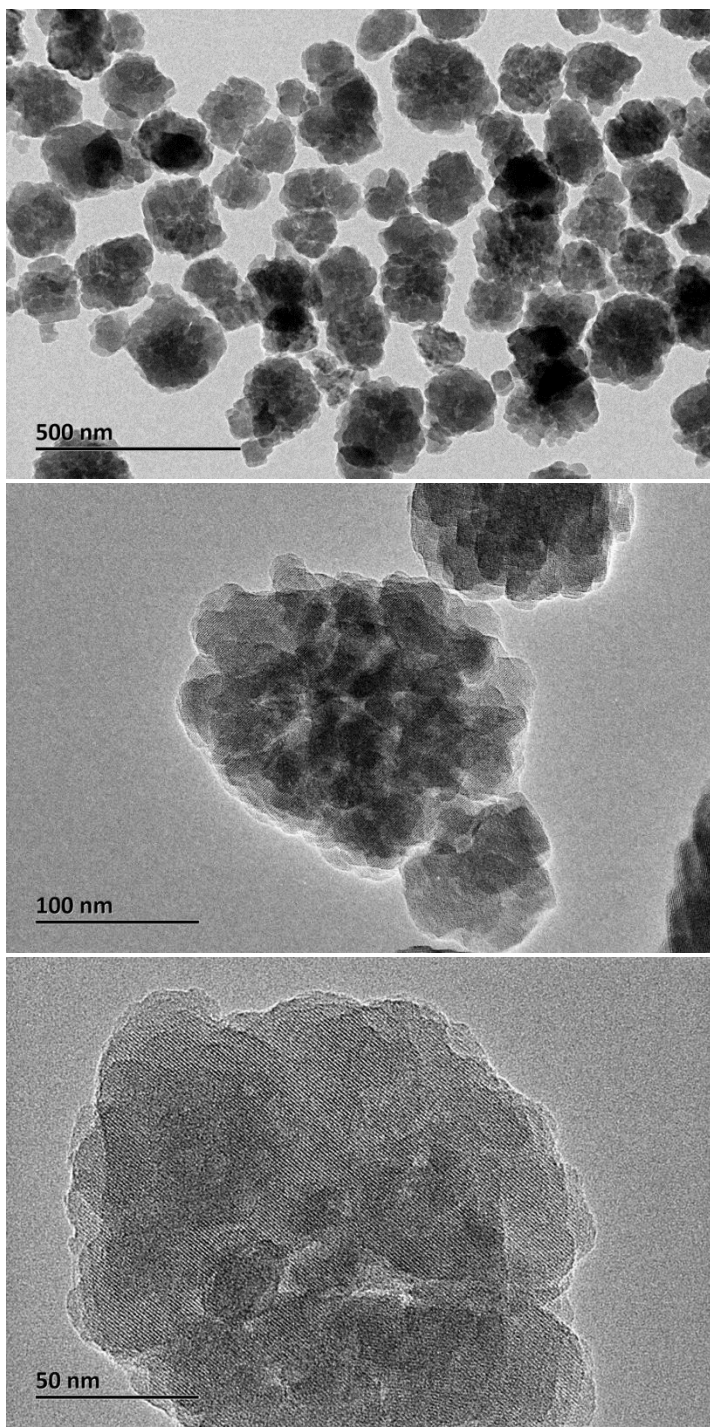


**Fig. S4** TEM images of the ZSM-5-2 crystallized at 180 °C for 3 h.

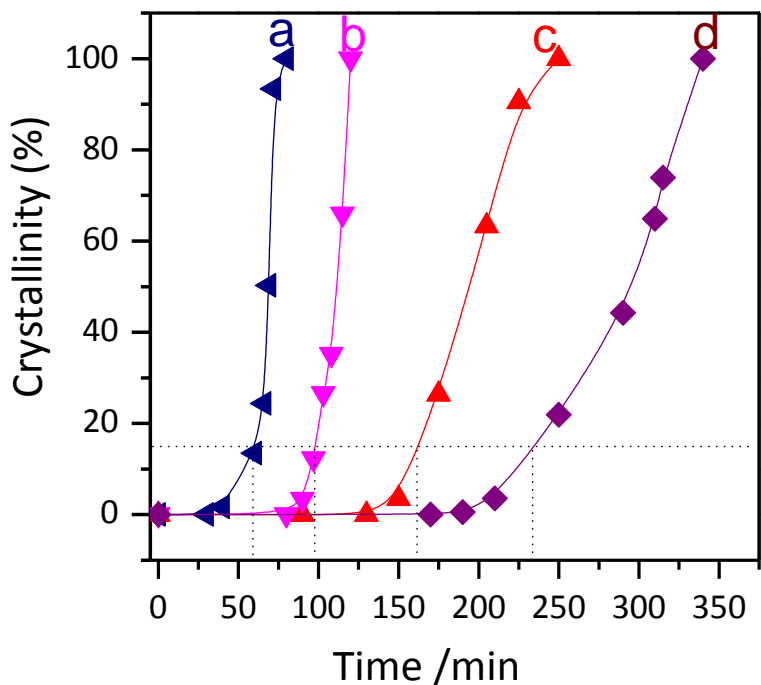


**Fig. S5** Dependences of the ZSM-5-2 crystallinity on the crystallization time synthesized at (a) 200 °C, (b) 180 °C, (c) 140 °C, and (d) 120 °C.

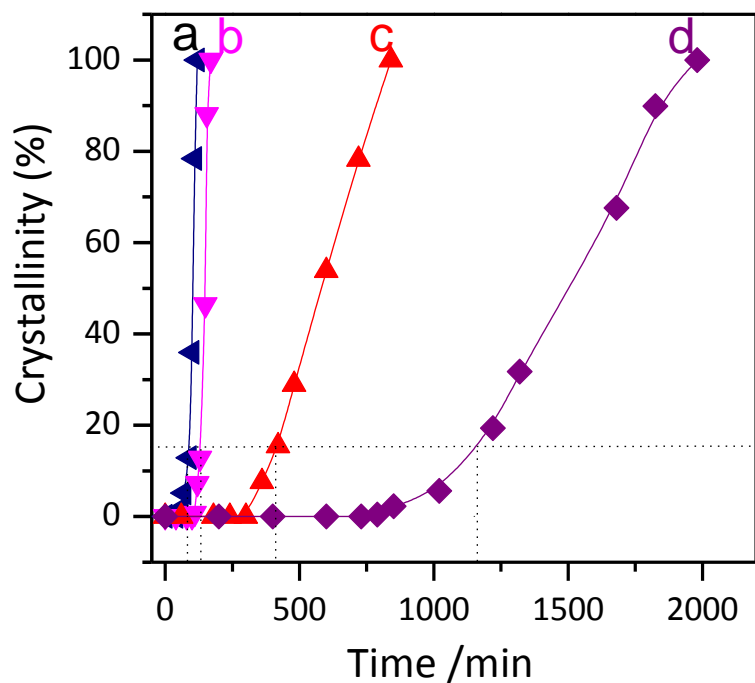


**Fig. S6** Dependences of the ZSM-5-10 crystallinity on the crystallization time synthesized at (a) 200 °C, (b) 180 °C, (c) 140 °C, and (d) 120 °C.

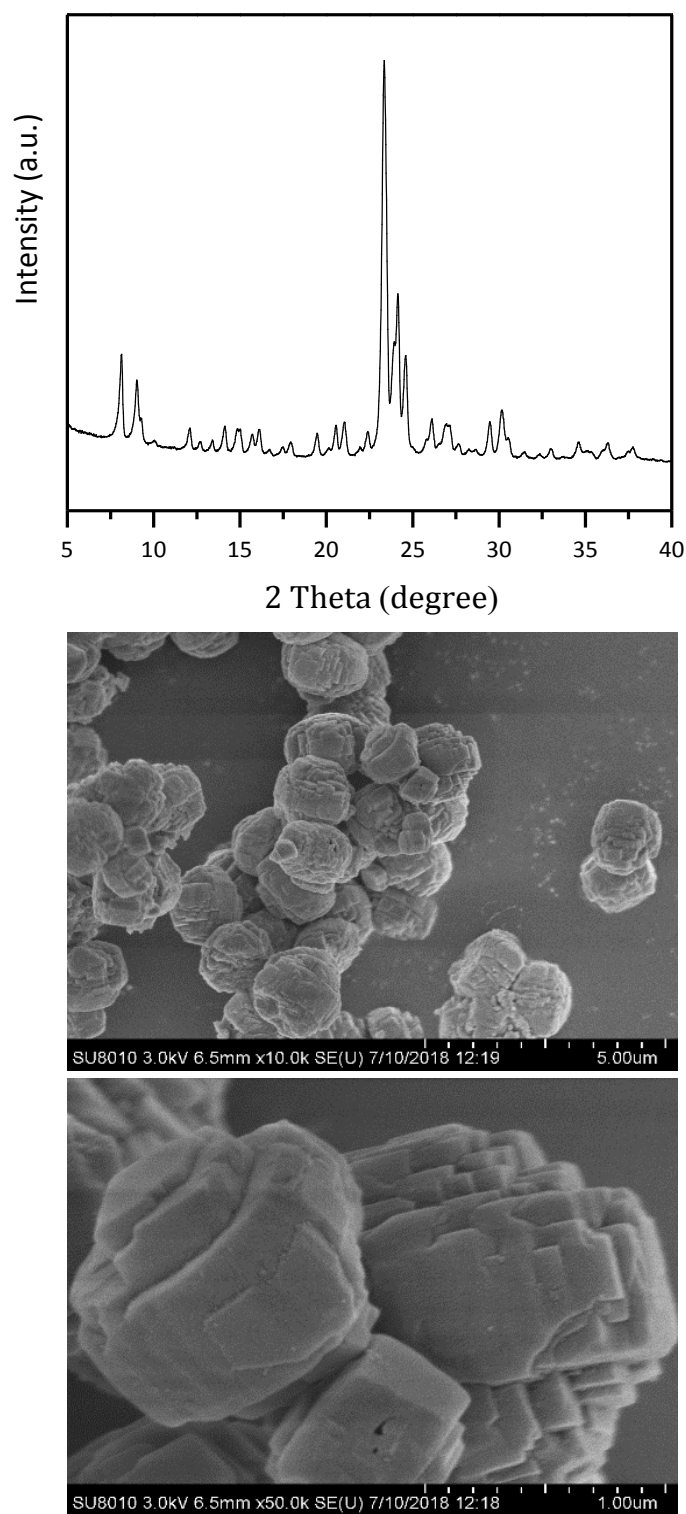


**Fig. S7** XRD pattern and SEM images of the ZSM-5-6 synthesized with additional NaOH (NaOH/SiO<sub>2</sub> at 0.15).

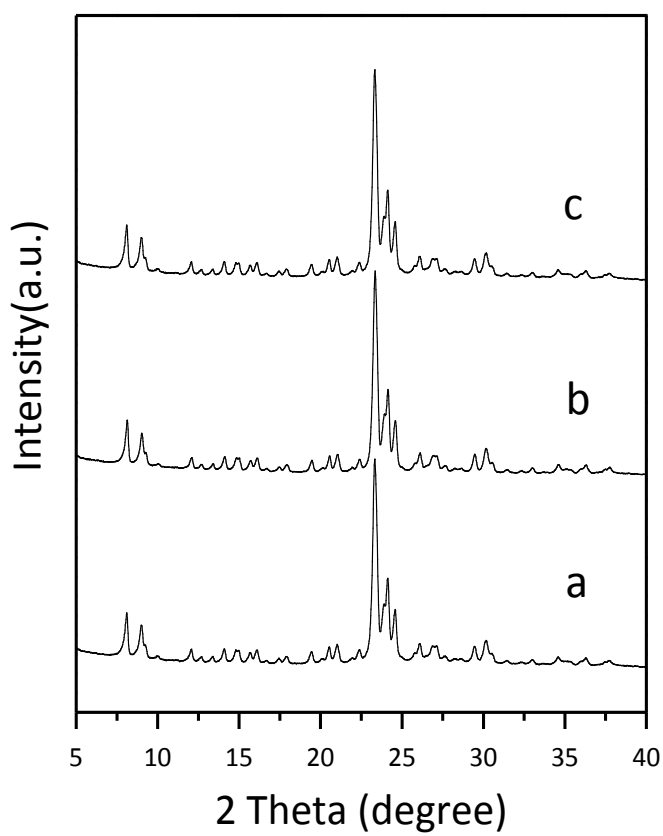


**Fig. S8** XRD patterns of the ZSM-5-2 zeolites synthesized in starting aluminosilicate gels with Si/Al ratio at (a) 100, (b) 200, and (c)  $\infty$ .

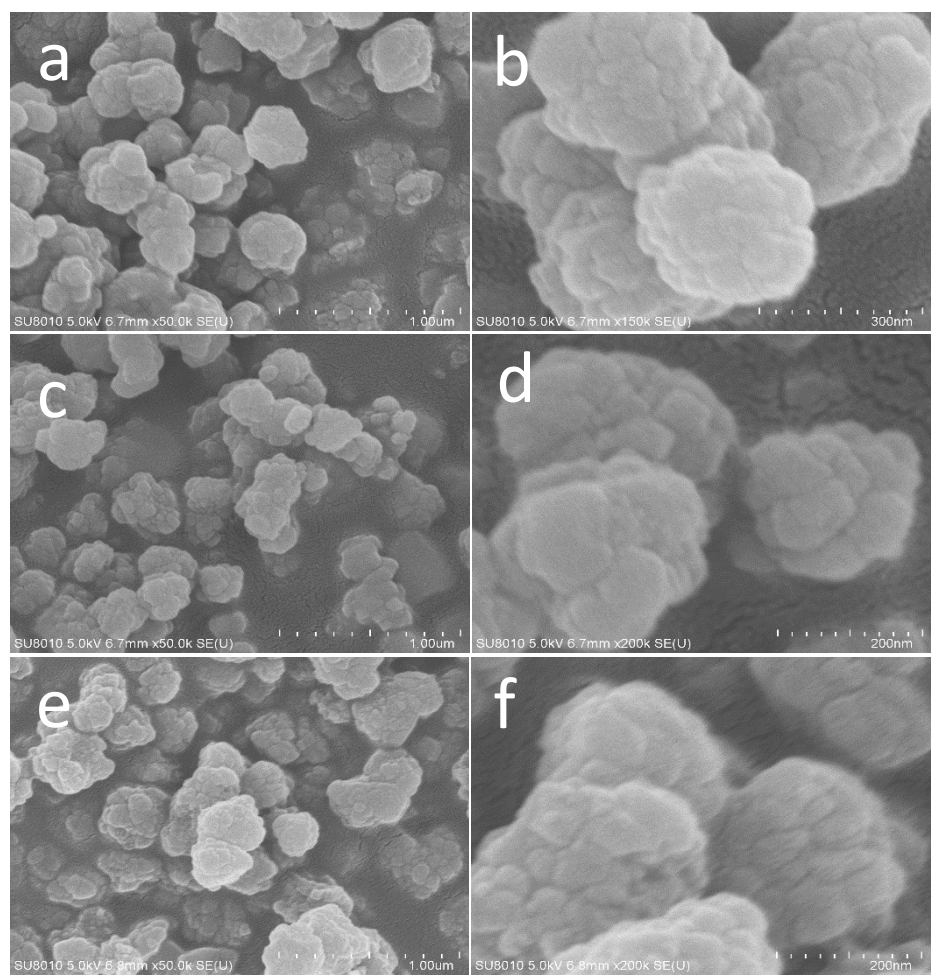


**Fig. S9** SEM images of the ZSM-5-2 zeolites synthesized in starting aluminosilicate gels with Si/Al ratio at (a) 100, (b) 200, and (c)  $\infty$ .

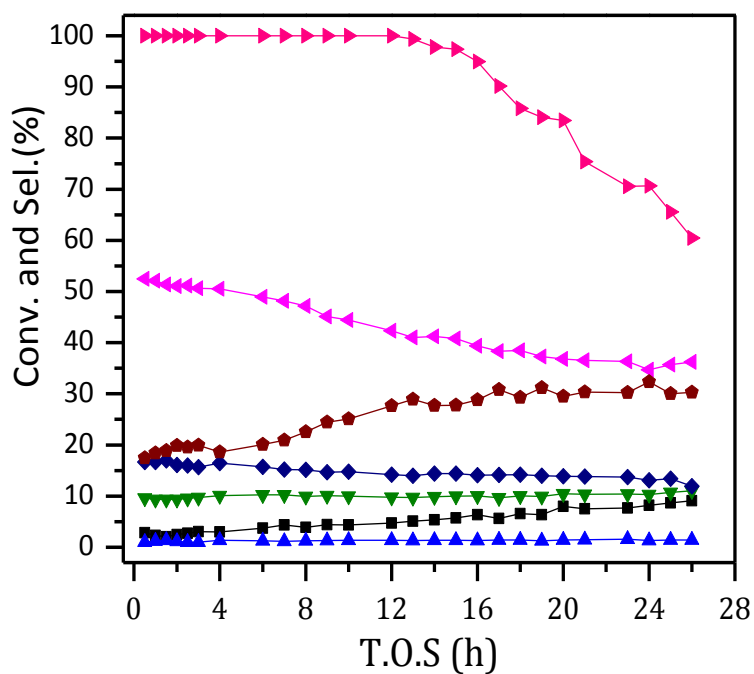


**Fig. S10** Dependences of catalytic conversion and product selectivity on reaction time in MTO over the conventional bulky ZSM-5 catalyst (C-ZSM-5, ▶Conv, ▼C<sub>2</sub><sup>±</sup>, ◀C<sub>3</sub><sup>±</sup>, ◆C<sub>4</sub><sup>±</sup>, ■C<sub>1</sub>, ▲C<sub>2-4</sub>, ♦≥C<sub>5</sub>).

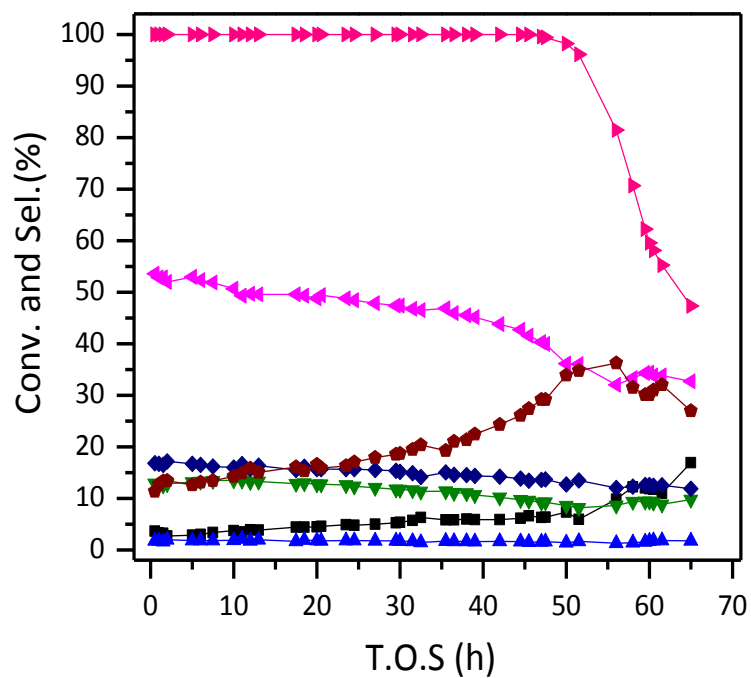


**Fig. S11** Dependences of catalytic conversion and product selectivity on reaction time in MTO over the CN-ZSM-5 catalyst (►Conv, ▼ $C_2^=$ , ▲ $C_3^=$ , ◆ $C_4^=$ , ■ $C_1$ , ▲ $C_{2-4}$ , ♦ $\geq C_5$ ).

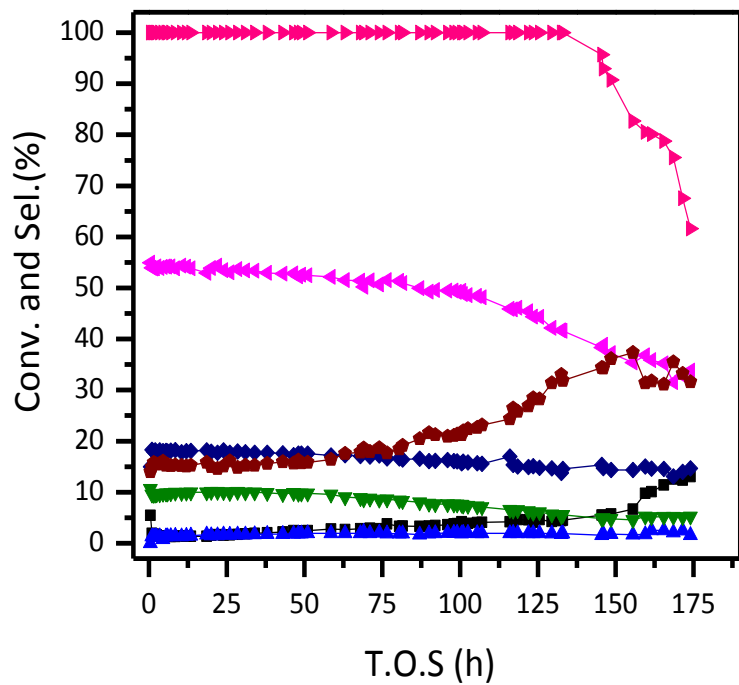


**Fig. S12** Dependences of catalytic conversion and product selectivity on reaction time in MTO over the ZSM-5-2 catalyst. (►Conv, ▼C<sub>2</sub><sup>=</sup>, ▲C<sub>3</sub><sup>=</sup>, ◆C<sub>4</sub><sup>=</sup>, ■C<sub>1</sub>, ▲C<sub>2-4</sub>, ♦≥C<sub>5</sub>)

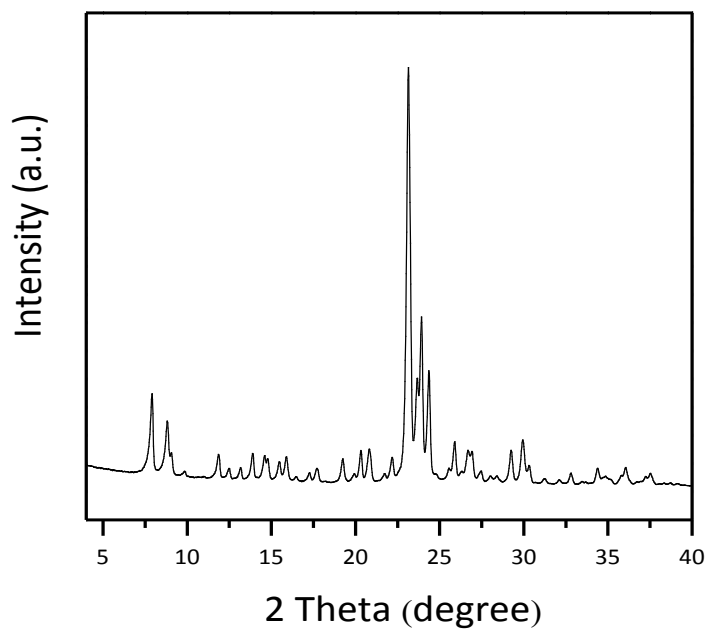


**Fig. S13** XRD pattern of CN-ZSM-5 zeolite from conventional hydrothermal route.

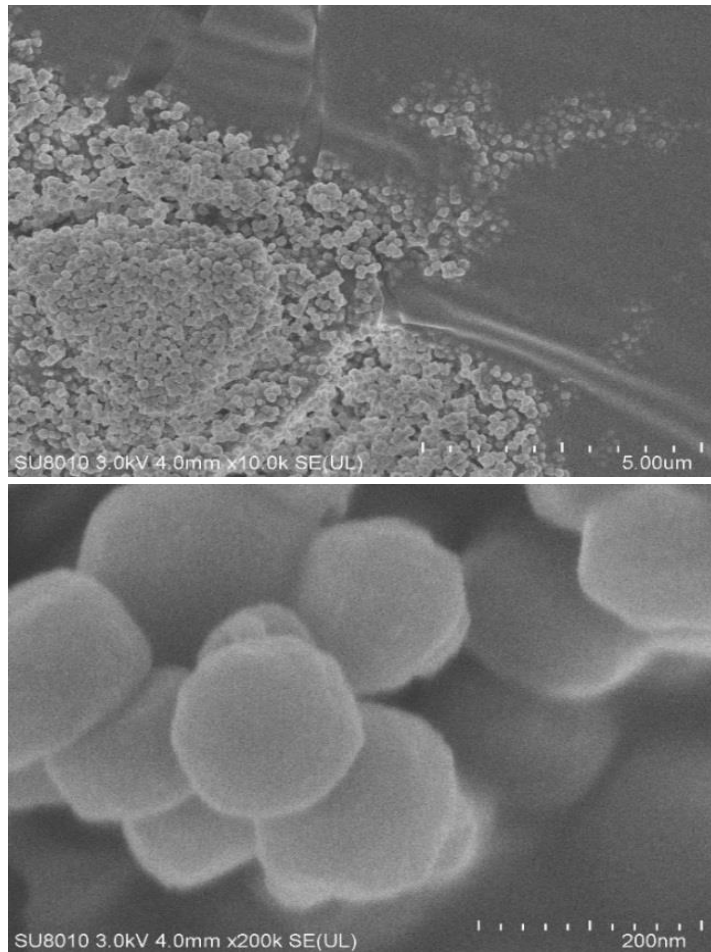


**Fig. S14** SEM images of CN-ZSM-5 zeolite from conventional hydrothermal route.

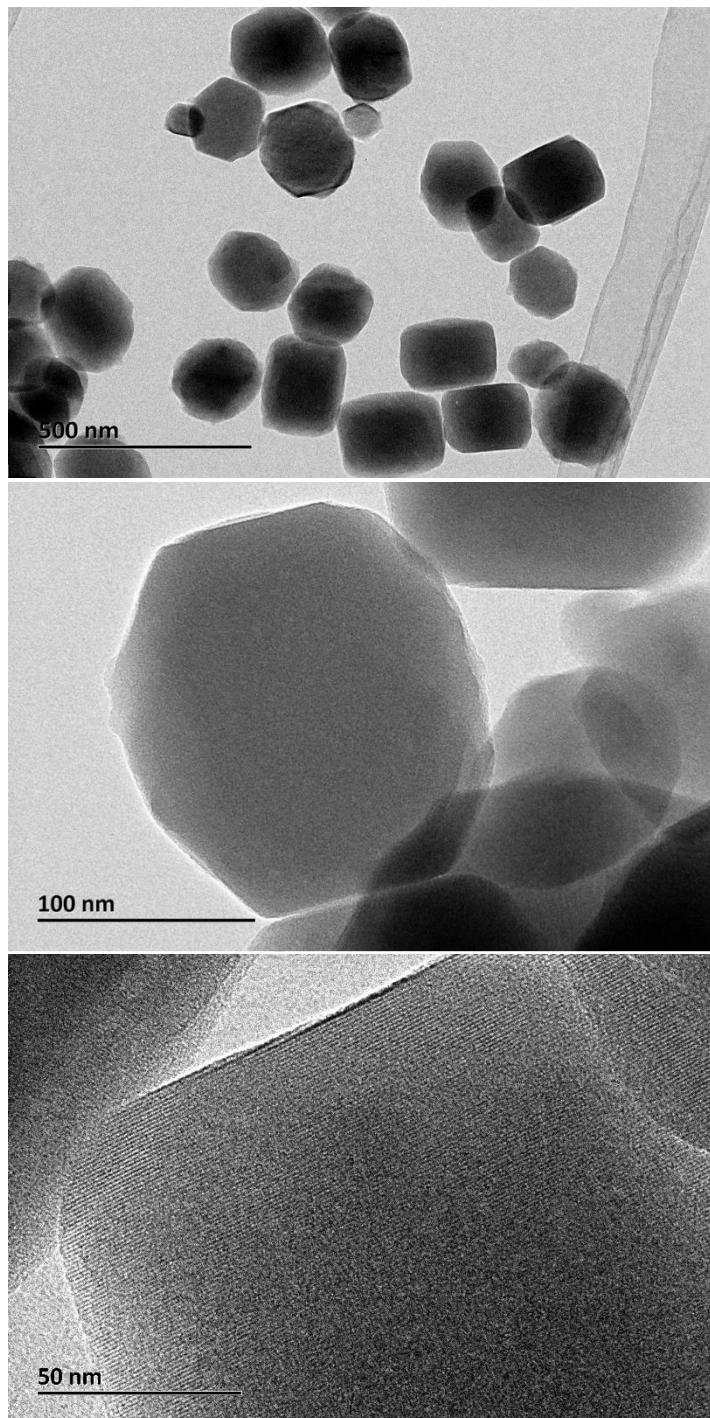


**Fig. S15** TEM images of CN-ZSM-5 zeolite from conventional hydrothermal route.

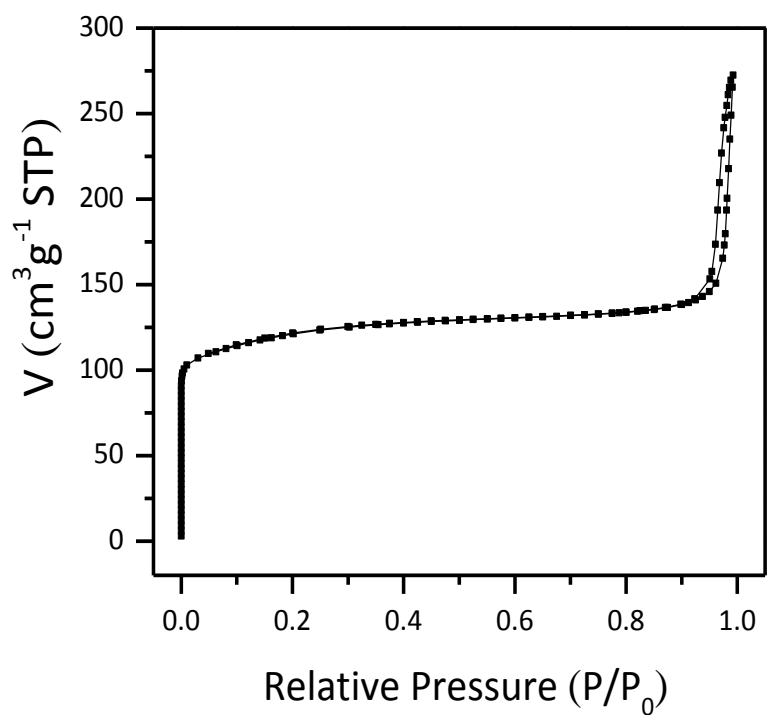


**Fig. S16** N<sub>2</sub> sorption isotherms of CN-ZSM-5 zeolite from conventional hydrothermal route.

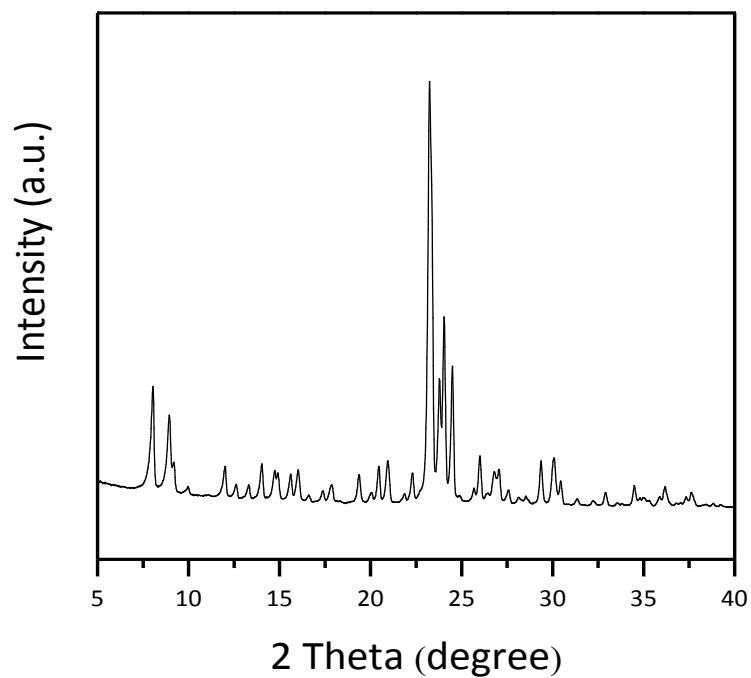


**Fig. S17** XRD pattern of the conventional bulky ZSM-5 zeolite.

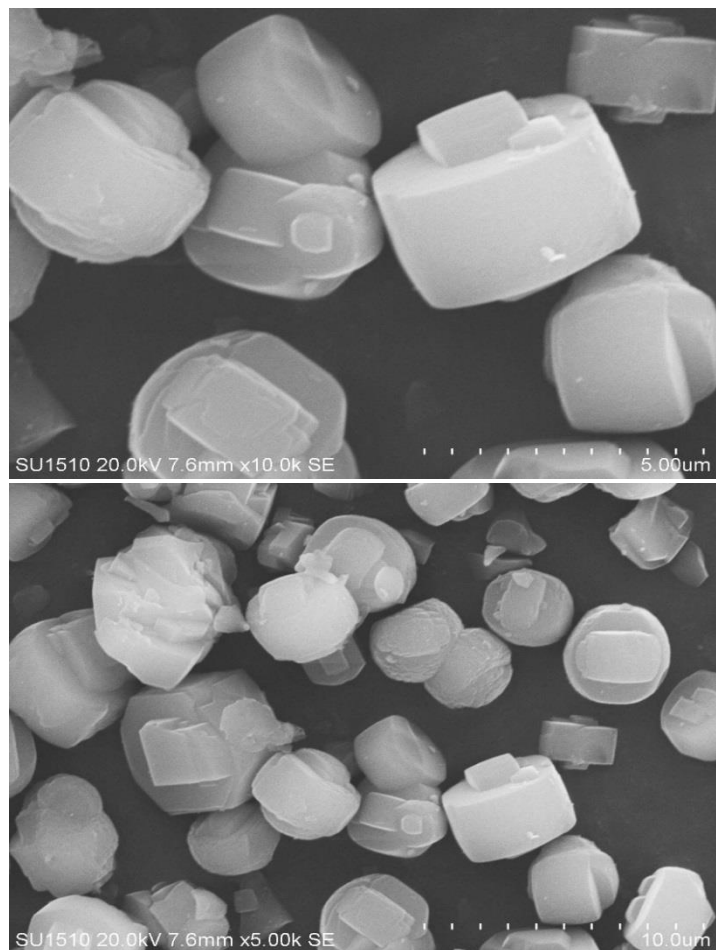


**Fig. S18** SEM images of the conventional bulky ZSM-5 zeolite.

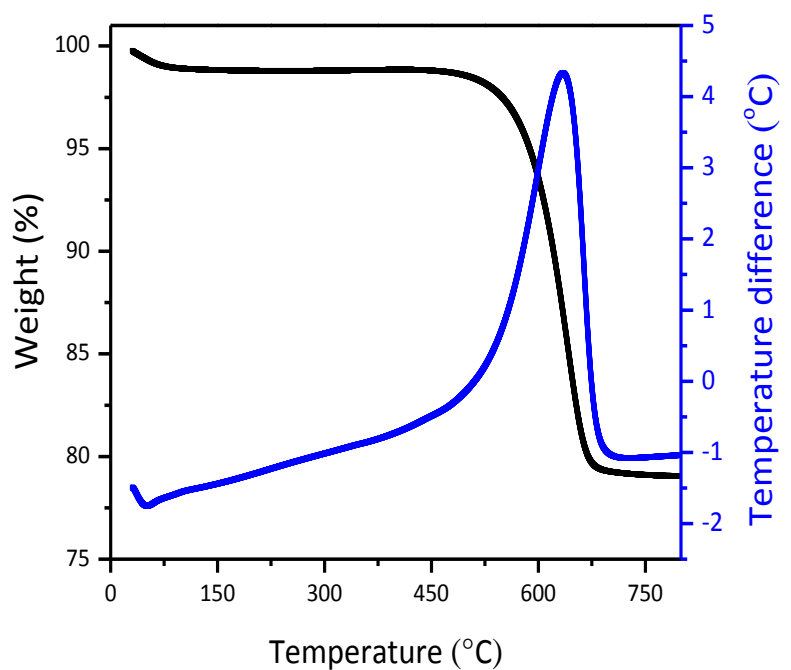


**Fig. S19** TG-DTA curves of the deactivated ZSM-5-2 catalyst.

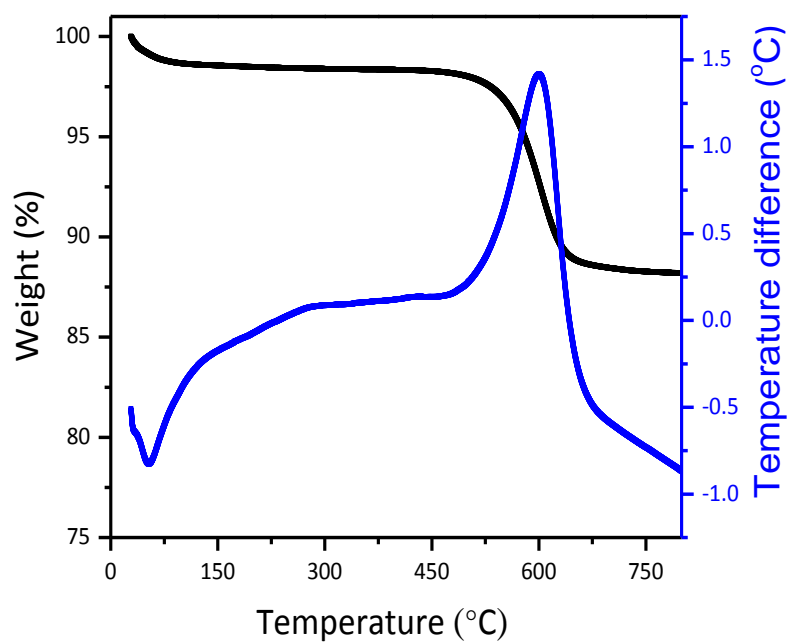


**Fig. S20** TG-DTA curves of the deactivated CN-ZSM-5 catalyst.

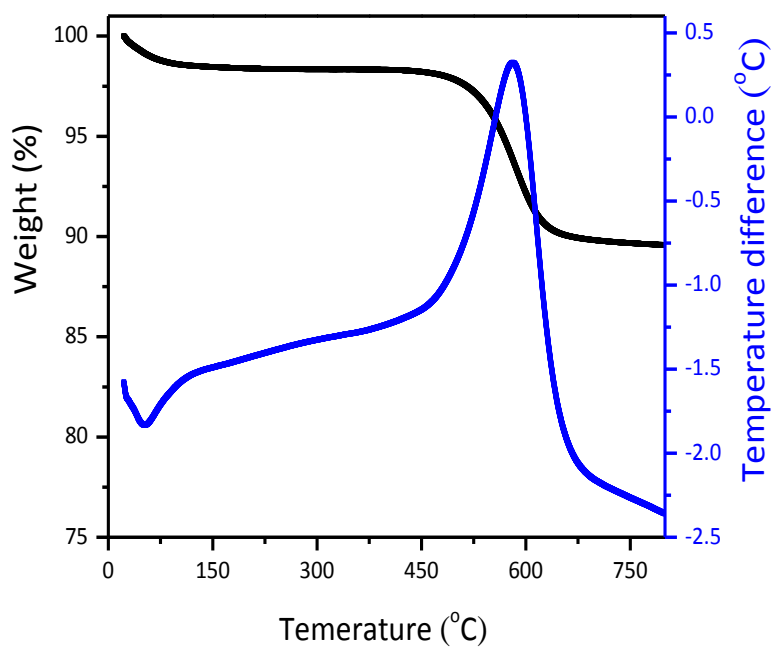


**Fig. S21** TG-DTA curves of the deactivated conventional bulky ZSM-5 catalyst.

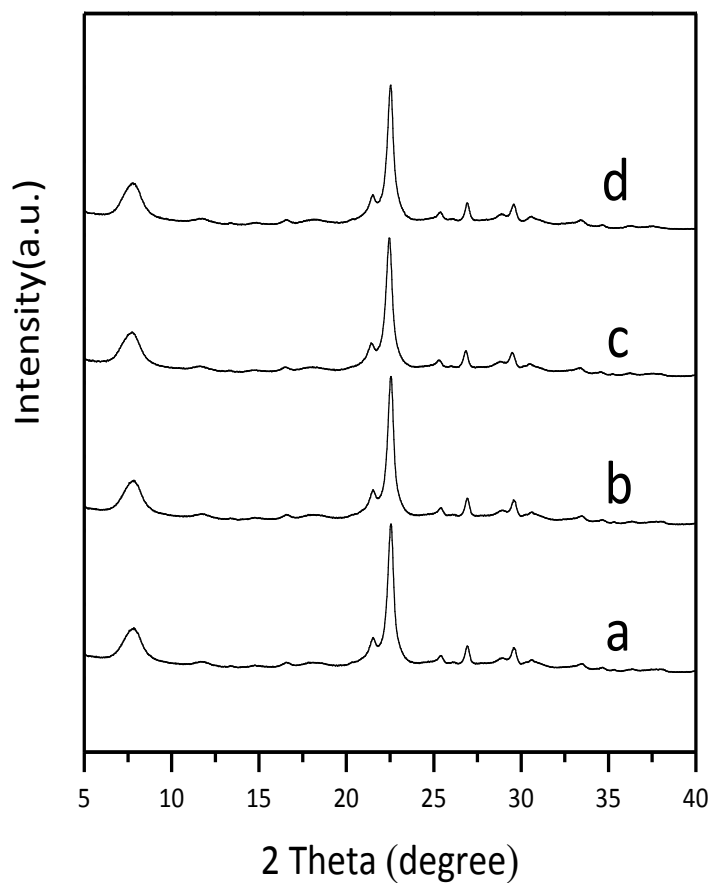


**Fig. S22** XRD patterns of the beta synthesized with  $\text{H}_2\text{O}/\text{SiO}_2$  ratio at (a) 2.50, (b) 3.75, (c) 5.00, and (d) 6.25.

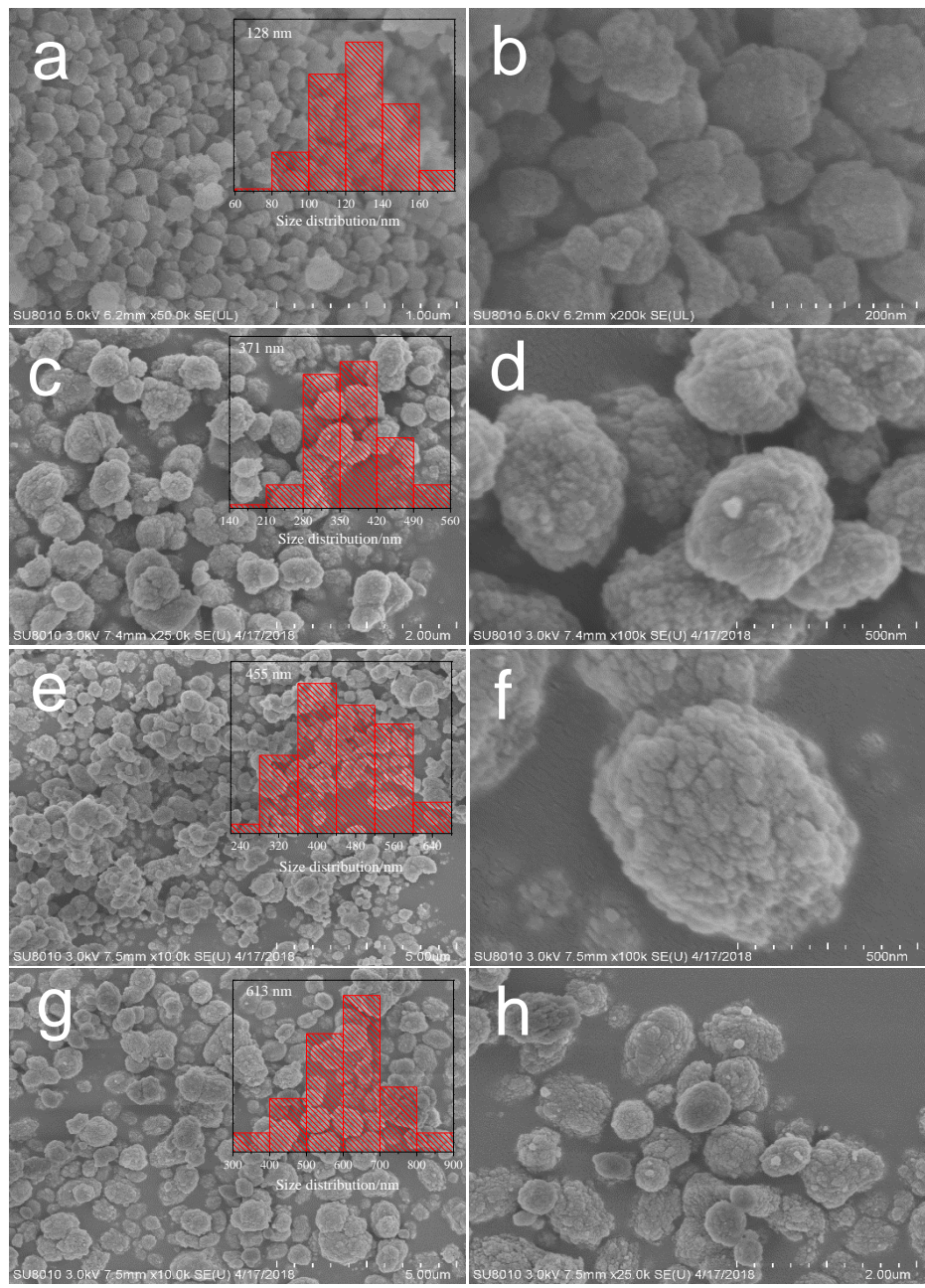


**Fig. S23** SEM images of the beta synthesized with  $\text{H}_2\text{O}/\text{SiO}_2$  ratio at (a,b) 2.50, (c,d) 3.75, (e,f) 5.00, (g,h) 6.25 (Size distribution of beta zeolites obtained by counting number of more than 200 zeolite particles in the SEM images).

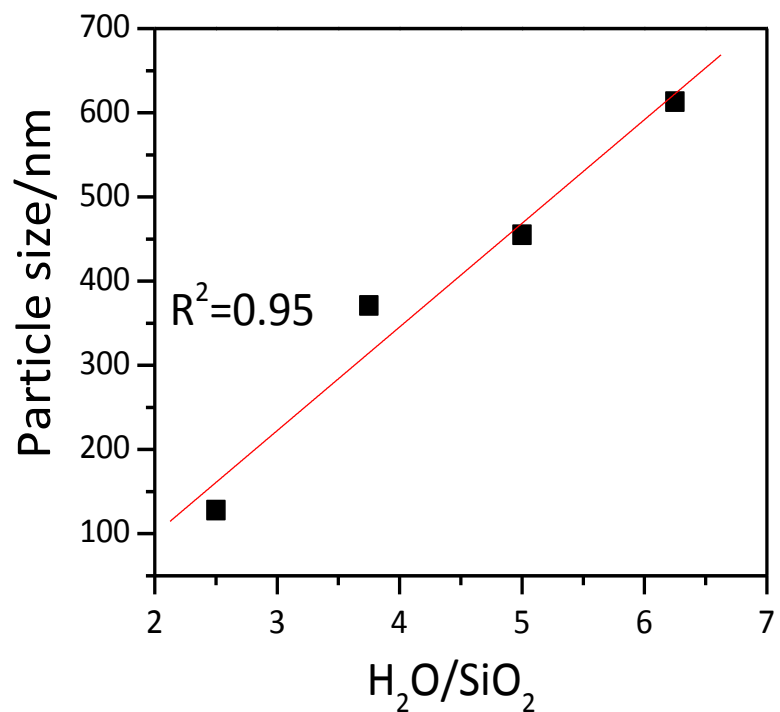


**Fig. S24** Dependence of obtained beta particle size on  $\text{H}_2\text{O}/\text{SiO}_2$  ratio.

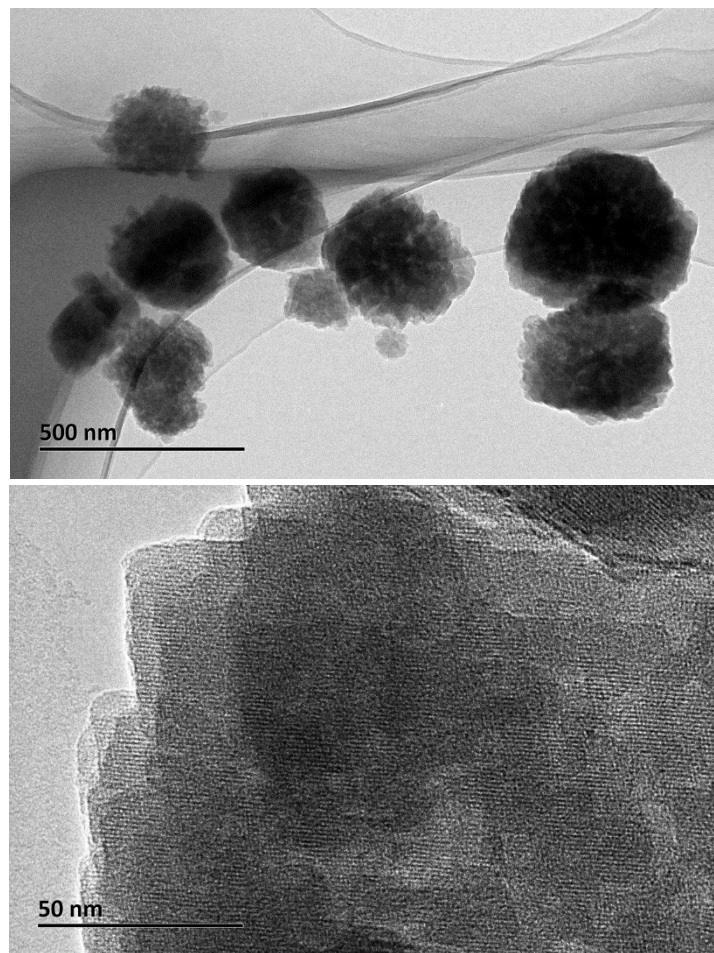


**Fig. S25** TEM images and SEAD pattern of Beta-2.5 zeolite.

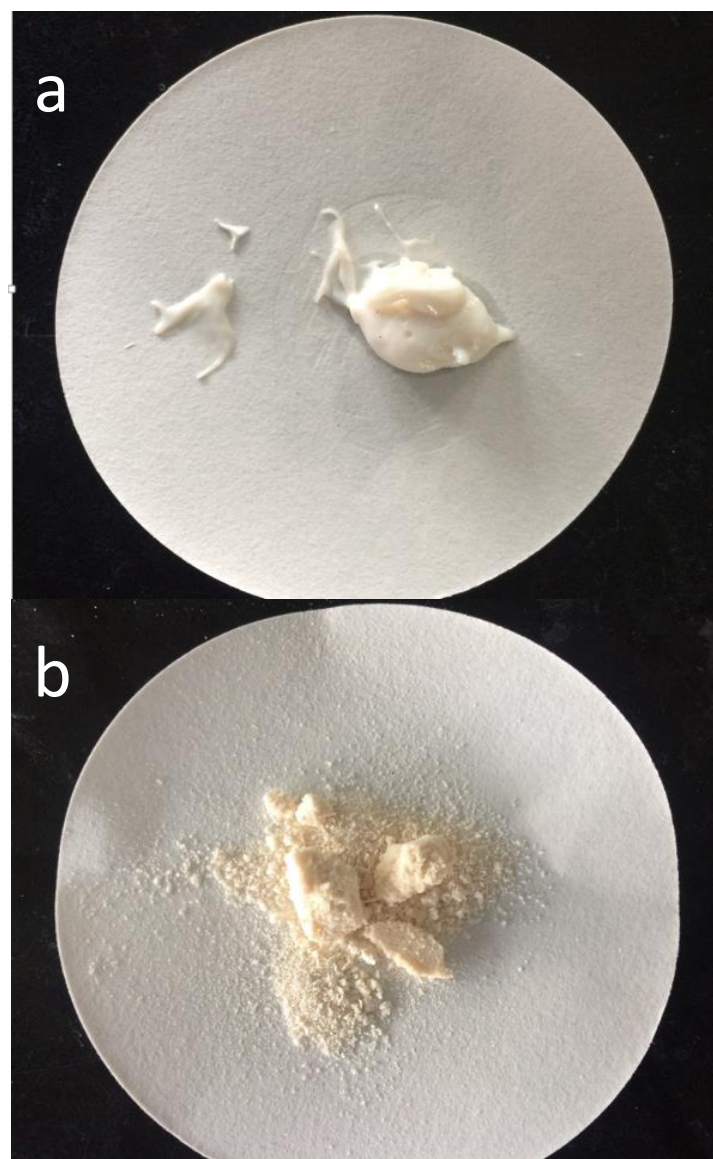


**Fig. S26** Photographs of fully crystallized (a) ZSM-5-2 and (b) Beta-2.5 zeolites.